Computational and Theoretical Chemistry 1024 (2013) 61–68

Contents lists available at ScienceDirect

Computational and Theoretical Chemistry

journal homepage: www.elsevier.com/locate/comptc

Structure and electronic properties of lithium–silicon clusters

Sebastián I. González [a], Ofelia B. Oña [b], Marta B. Ferraro [a], Julio C. Facelli [c,d,*]

[a] Departamento de Física, Facultad de Ciencias Exactas y Naturales, Universidad de Buenos Aires and IFIBA, CONICET, Argentina
[b] Instituto de Investigaciones Fisicoquímicas Teóricas y Aplicadas, Universidad Nacional de La Plata, CCT La Plata, CONICET, Sucursal 4, CC 16, 1900 La Plata, Argentina
[c] Department of Biomedical Informatics, University of Utah, 155 South 1452 East Rm 405, Salt Lake City, UT 84112-0190, USA
[d] Center for High Performance Computing, University of Utah, 155 South 1452 East Rm 405, Salt Lake City, UT 84112-0190, USA

ARTICLE INFO

Article history:
Received 30 July 2013
Received in revised form 16 September 2013
Accepted 17 September 2013
Available online 27 September 2013

Keywords:
Genetic Algorithms
Lithium-Silicon Clusters
Endohedral Lithiation

ABSTRACT

This paper reports results of global searches of the most stable structures of silicon–lithium clusters for the series Si_nLi (n = 2–12) using parallel Genetic Algorithms (GA). For this study we have used our MGAC software directly coupled with DFT energy calculations (MGAC/CPMD). The paper reports the stable geometries, binding energies, HOMO–LUMO gap, and electronic properties at the PBE/6-311G(2d) level of theory. Global searches did not find any endohedral Si_nLi structures, which we find as local minima with energies much higher than most of the stable Si–Li clusters found by MGAC/CPMDGenetic.

1. Introduction

Silicon is the most common element used in microelectronic components; therefore Si clusters have been studied extensively from the experimental [1–3] and theoretical [4–6] points of view. The characterization and prediction of the structures of metal silicon clusters is also important for nanotechnology because these clusters can be used as building blocks for multiple applications [7–11]. Alkali metal silicon clusters are interesting because of their utility in catalysts, as materials for aircrafts and other products like zeolites, glasses and ceramics. There is also a great interest in the developing of high-performance lithium battery anodes using silicon nanowires [12]. Silicon is an attractive anode material because it has a low discharge potential and high theoretical charge capacity (4200 mAh g^{-1}) [13]. The disadvantage is that silicoń s volume increases by 400% by insertion and extraction of lithium [14], resulting in capacity fading. Chan et al. [12] proved that silicon nanowire electrodes can accommodate strain without pulverization with good contact and conduction and displaying short lithium insertion distances. The geometric dependence of the current–voltage (I–V) has been investigated employing silicon hydrogenated nanowires between lithium electrodes [15], but still it is unclear if the existence of endohedral Li–Si structures may be an impediment for using these Si nanowires as electrodes in lithium batteries.

Examples of studies of the structure and properties of alkali metal silicon clusters are given in the following publications: Kaya et al. [16–18] have provided experimental and theoretical data of ionization potential and electron affinities of sodium doped silicon clusters. Zubarev et al. [19] employed photoelectron spectroscopy to measure the electron affinity of Si_6Na. Lin et al. [20] studied Si_nLi ($n \leqslant 10$) clusters and their anions employing different methods of density functional theory (DFT). Wang et al. [21] employed the QCISD/6-311+G(d,p)//MP2/6-31G(d) approach to study Si_nLi (n = 2–7) clusters. Rabilloud et al. [22–24] reported the equilibrium geometries and electronic properties of Si_nLi_p ($n \leqslant 6$, $p \leqslant 2$) and $Si_nLi_p^{(+)}$ ($n \leqslant 6$, $p \leqslant 2$) at MP2 and DFT levels, and the charge transfer [24] from the alkali atom to silicon and their relation with the dipole moment in Si_nM_p (M = Li, K, Na). Hao et al. [25] performed higher level of *ab initio* calculations to study electronic properties of Si_nLi^- (n = 2–8) clusters, as electron affinities and dissociation energies, employing the Gausian-3 (G3) theory [26]. In all these studies the optimized geometries of the clusters have been obtained by local optimizations of starting structures assembled by *substitution* of a silicon atom in a Si_n^{+1} cluster by a Li^-, or by attaching a Li^- into a Si_n^+ cluster. Very recently, Koukaras et al. [27] explored the possibility of designing relatively stable (viable) lithiated silicon fullerenes of high symmetries, which are characterized by large hyperpolarizabilities. They showed that the $Si_{20}Li_{20}$ fullerene like structure is a highly hyperpolarizable cluster because the lithiation is responsible for a rich region of electronic excitations associated with low excitation energies and intense transitions. Ionization energies and structures of Si_nLi_m (n = 5–11, m = 3–6) were reported and discussed in a combined experimental

* Corresponding author at: Center for High Performance Computing, University of Utah, 155 South 1452 East Rm 405, Salt Lake City, UT 84112-0190, USA.
E-mail address: Julio.Facelli@utah.edu (J.C. Facelli).

2210-271X/$ - see front matter © 2013 Elsevier B.V. All rights reserved.
http://dx.doi.org/10.1016/j.comptc.2013.09.019

and theoretical study by De Haeck et al. [28]. They showed that subsequent addition of lithium causes electron excess in the silicon framework, which produce a decrease of the ionization energy with the increase of lithiation. The excess of lithiation for the case of Si_4 clusters and its relation with the morphology of the silicon framewrok has been studied by Osorio et al. [29]. In spite of all this work to the author's knowledge no global search techniques have been used to study possible structures of alkali metal silicon clusters and therefore the energetics of the endohedral Li–Si cluster is not clear understood [30].

In order to have a better insight into the possibility of insertion of lithium in silicon electrodes, or a transition between *exo* to *endo* absorption of lithium in Si_nLi clusters we have performed a global search of Si_n–Li structures employing our Parallel Genetic Algorithms (PGA) [31,32] as implemented in our MGAC software [33–35], directly coupled with DFT local optimizations and energy calculations. Previously, we have been able to find energetically favorable endohedral structures for $CuSi_{10}$ [36], without any *a priori* assumption of their existence, i.e., they were found automatically by the GA search. The existence of a similar transition from *exo* to *endo* insertion of lithium in Si_n clusters would be a severe disadvantage when building nanowires that are chemically stable and weakly interacting.

2. Methods

GA methods are based on the principle of survival of the fittest; in order to determine the most stable isomers, considering that each string or genome represents a set of trial solutions candidate (cluster structures) that at any generation compete with each other in the population for survival and produce offspring for the next generation by prescribed propagation rules. In this work we follow the protocols used in our previous studies of Si and Cu–Si clusters [32,36]. The clusters are represented by a genome of dimension 3*N*, where *N* is the number of atoms in the cluster, the genetic operators, mating, crossover, mutation, etc., have been constructed in such way that when they are applied to the genome they produce a valid individual, i.e., a possible structure of a cluster of the desired size. The GA operations of mating, crossover, and the "cut and slice" operator introduced by Johnston and Roberts [37] are used here to evolve one generation into the next one. The best individuals among the population, 50%, are directly copied into the next generation, and the other 50% are replaced applying the genetic operators. This technique is also known as elitism. The criteria for fitness probability, selection of the individuals and genetic operators are discussed in detail in Ref. [38]. The GA procedure was run several times to guarantee that the resulting structures are independent of the initial population. We ran the MGAC three times per Si_nLi system, employing from 15 to 200 generations with 10 individuals. The total number of computer processors employed for each run ranged from 49 to 98.

All the energy calculations were done using the CPMD code [39]. The isomers selected by MGAC/CPMD calculations were analyzed, and their vibration frequencies evaluated to discriminate transition states (*TS*) from stable structures. In this study we used the Goedecker et al. [40] pseudopotential, the PBE (Perdew–Burke–Ernzerhof) [41] exchange correlation functional with an energy cutoff (Ecut) of 70 Ry, and a cell length of 4.5 Å plus the largest dimension of the cluster. The Ecut was selected by the usual procedure, it was varied between 5 and 105 Ry and the energy convergence was achieved at 70 Ry. The pseudopotential was selected after comparing the RMS (root mean square) between experimental and predicted bond lengths, binding energies, and vibrational frequencies for Si_2, Li_2, Si_2Li, Si_3Li and Si_4Li, employing different density functional methods implemented in the CPMD code and B3LYP/6-311G(2d) all electron method implemented in Gausian03 [42]. The results of this comparison are presented in Table 1, which shows that the selected combination is as good or better than any other DFT approach and better than most of the all electron approaches considered here.

In this paper we have also evaluated the static dipole polarisabilities, inertial moments, alpha and beta gaps, the binding energies per atom (E_b/atom) as a function of the number of silicon atoms, adiabatic ionization energies (AIEs), electron affinities (APEs) and frequencies for each Si_nLi (n = 2–10, 12) final most stable structure at the PBE/6-311G(2d) level of theory using the Gaussian03 package of programs [42]. AIEs have been compared with experimental values taken for Ref. [43].

3. Results and discussion

Table 1 reports the RMS (root mean square) between the bond lengths *in* Li_2, Si_2, SiLi, $SiLi_3$, $SiLi_4$, and bond angles in $SiLi_3$ and $SiLi_4$, calculated for different combinations of pseudopotentials and functionals tested to choose the DFT level of theory that was selected for the GA global optimizations and their corresponding experimental and/or all electron calculations. From this analysis we chose the combination GO_PBE to perform the Si–Li predictions as the best performing.

Fig. 1 shows the most stable structures for Si_nLi (n = 2–7) clusters with doublet spin symmetry obtained by the MGAC/CPMD global optimizations. The structures of Si_nLi for n = 8, 9, 10, 12 are depicted in Figs. 2–5, respectively. These structures were symmetrised and re-optimized at the PBE/6-311G(2d) level to look for imaginary frequencies. The label (*TS*) indicates that the isomer is a transition state at this level of theory. Those structures enclosed

Table 1
RMS (root mean square) between the bond lengths in Li_2, Si_2, SiLi, $SiLi_3$, $SiLi_4$, and bond angles in $SiLi_3$ and $SiLi_4$, calculated for different combinations of pseudopotentials and functionals tested to choose the DFT level of theory that was selected for the GA global optimizations and their corresponding experimental and/or all electron calculations. A energy cutoff, E_{cut} = 70 Ry was used in these calculations.

Method	Li_2[a]	Si_2[a]	Si–Li[b]	Si_2Li[b]		Si_3Li[b]		Si_4Li[b]		RMS (Å)	Δ (°)
	RMS (Å)	RMS (Å)	RMS (Å)	RMS (Å)	Δ (°)	RMS (Å)	Δ (°)	RMS (Å)	Δ (°)		
GO_PBE	0.001	0.032	0.002	0.001	0.013	0.007	0.391	0.007	0.215	0.004	0.089
GO_LDA	0.001	0.008	0.011	0.014	0.100	0.016	0.157	0.017	0.535	0.006	0.193
SG_LDA	0.001	0.008	0.011	0.014	0.100	0.016	0.157	0.017	0.535	0.006	0.193
GO_BP	0.001	0.028	0.025	0.008	0.193	0.009	0.361	0.007	0.204	0.010	0.077
GO_PADE	0.001	0.008	0.060	0.037	0.487	0.025	0.162	0.021	0.554	0.019	0.172
GO_BLYP	0.001	0.034	0.084	0.044	0.776	0.038	2.161	0.008	0.195	0.027	0.825
SG_BLYP	0.001	0.034	0.088	0.043	0.797	0.037	2.114	0.008	0.210	0.028	0.796
MT_BLYP	1.973	0.218	0.252	0.161	1.061	0.146	1.012	0.091	0.918	0.673	0.059

[a] RMS between CCCBDB NIST [47] database and CPMD results.
[b] RMS between optimized bond lengths at the B3LYP/6-311G(2d) and CPMD results for those systems with no experimental data in the literature.

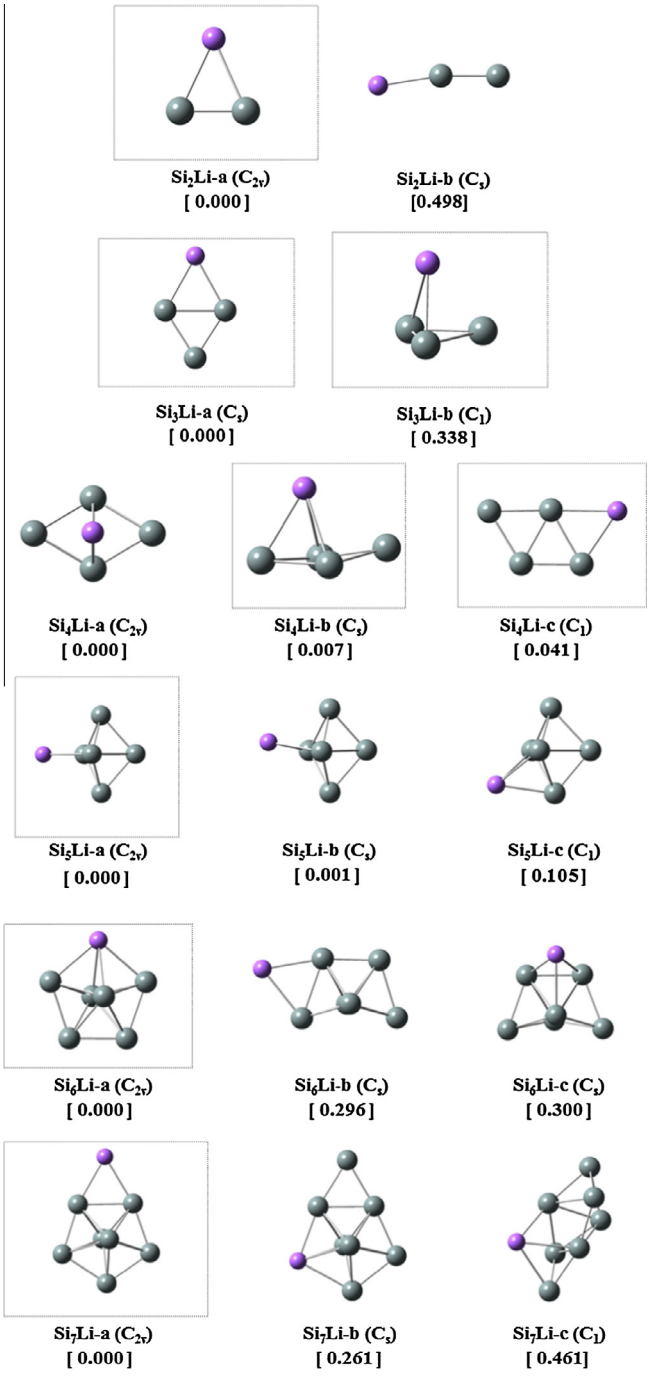

Fig. 1. Si_2Li–Si_7Li structures obtained by the MGAC/CPMD and relative energies in eV.

into frames have been previously reported by other authors [21,25]. For each system the relative energies with respect to the most stable structure are also reported in the figures. The energies are expressed in eV. The bond lengths for Si_nLi (n = 2–10, 12) clusters predicted by the MGAC/CPMD method are reported in Tables 2 and 3, respectively. The adiabatic ionization energies (AIPs) and adiabatic electron affinities (AEAs) are reported in the same tables. The AIPs compare successfully with the experimental and calculated results reported in Ref. [43].

The anions corresponding to the structures in Figs. 1–5 are displayed in Fig. I-a of Supplementary material section. The were obtained by adding an electron to the neutral cluster and re-optimizing the structure at the PBE/6-311G(2d) level of theory.

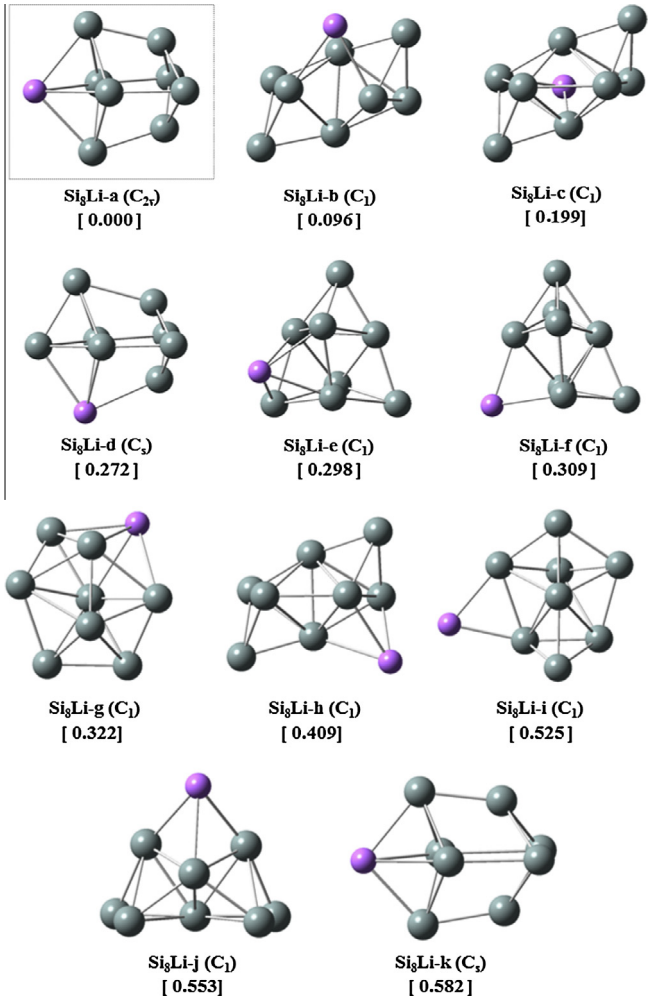

Fig. 2. Si_8Li structures obtained by the MGAC/CPMD and relative energies in eV.

The same procedure was used to obtain the structures of the corresponding singly charged Si_nLi^+ clusters, which are shown in Fig. I-b of the Supplementary material. The charged species corresponding to n = 8 (9, 10 and 12) are reported in Figs. II-a and II-b (III-a and III-b, IV-a and IV-b and, V-a and V-b) of Supplementary material. Singlet and triplet spin symmetry was considered for charged clusters, but only Si_2Li^+ and some isomers of the Si_3Li^+ and Si_8Li^+ clusters have triplet spin symmetry: Si_2Li^+-a, Si_2Li^+-b, Si_3Li^+-a, Si_8Li^+-i and Si_8Li^+-g.

Si_2Li-a, has C_{2v} symmetry, as it was reported in the bibliography [21]. Si_2Li-b differs from the structure from Ref. [22], because the atoms are not on a straight line. Actually the structure from Sporea et al. [22] is 1.5 eV above the energy of our most stable cluster, and has two imaginary frequencies for our level of theory. The anion structures for Si_2Li^- do not differ from their neutral parent; therefore, we report only the most stable one (previously reported in Ref. [44]) in Fig. I-a. The cation structures interchange their energy ordering with respect to the neutral isomers, and the -b one corresponds to the straight line structure previously found in the literature [22]. It is also observed that the Si–Li bond length increases by 0.209 Å and 0.170 Å from its values in the neutral -a and -b isomers, respectively.

Si_3Li-a and Si_3Li-b were both previously reported in the literature [25]. The Si_3 frame of both isomers is identical to that of Si_3 and the most stable one (-a) shares its structure with Si_4, both reported in Ref. [32]. The anion structures do not change respect to

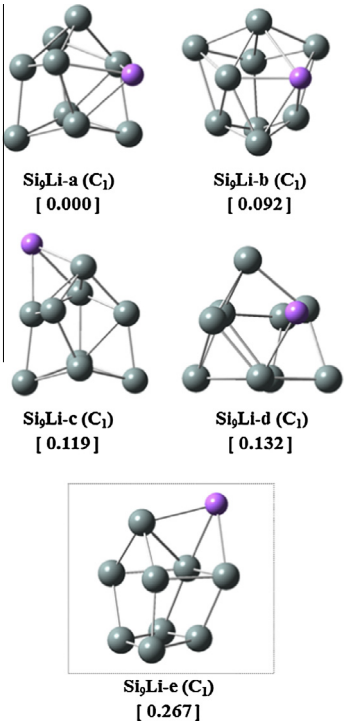

Fig. 3. Si_9Li structures obtained by the MGAC/CPMD and relative energies in eV.

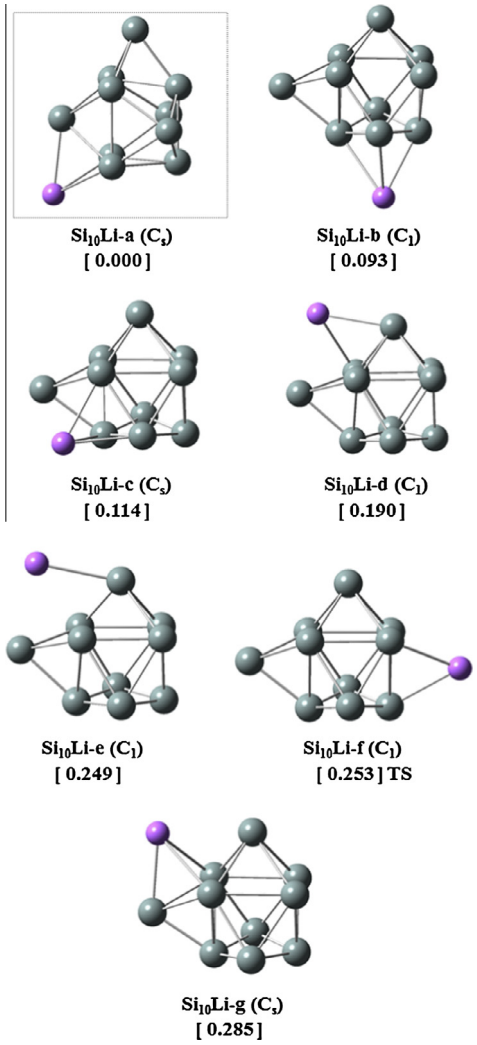

Fig. 4. $Si_{10}Li$ structures obtained by the MGAC/CPMD and relatives energy in eV.

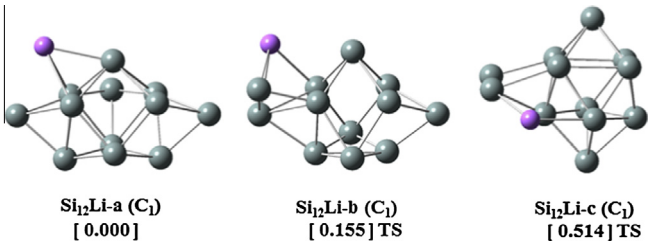

Fig. 5. $Si_{12}Li$ structures obtained by the MGAC/CPMD and relatives energies in eV.

the neutral ones, and were also previously reported [25]. The cation structures interchange their ordering with respect to the corresponding neutral isomers, but in the case of the b isomer, the lithium atom is bonded to only one silicon atom. The Si–Li bond length increases by 0.179 Å and 0.090 Å with respect to the neutral isomers.

We found a new neutral isomer, Si_4Li-a, not previously reported in the literature, which is 0.007 eV more stable than Si_4Li-b, which has been found in previous theoretical studies that also found the Si_4Li-c cluster [21,22,24,25]. We made the zero point correction, at the same level of accuracy, for isomers a and b, and their relative energy went from 0.007 eV to 0.006 eV, confirming a very low energy barrier. We checked the ordering between those isomers at CCSD/6-311G(2d) level, and confirmed again the PBE/6-311G(2d) findings with a relative energy of 0.03 eV between isomers a and b. The energy of these three, a, b, and c, structures differs in no more than 0.05 eV and the corresponding anions show the same symmetry than the neutral clusters but their energy ordering is interchanged. This finding is important since Yang et al. [44] assumed that the anion reported here as "-b", was very different from the neutral one. The Si–Li bond length is 2.612 Å for the neutral isomers and 2.481 Å for the anions. The relative energy order of the corresponding positive charged clusters differs from that of neutral species, and only the two depicted structures in Fig. I-b in Supplementary materialremain stable after ionization. Sporea et al. [22] checked relative energy order by single-point CCSD(T)/6-31+G(d) calculations; in this case, the Li atom in the cation systems are slightly displaced of their respective neutral clusters and the order of the energies is the same exhibited by the neutral clusters.

Our lowest energy neutral isomer Si_5Li-a is not stable and matches Wang et al. [21] MP2 structure with C_{2v} symmetry and one imaginary frequency. We also found two more higher energy isomers, Si_5Li-b and Si_5Li-c, both stable, and not previously reported in the literature, with C_s and C_1 symmetry, respectively. The "-a" and "-b" isomers have quite similar energies, but as stated before -a is not a local minimum at our level of theory. The Si_5 frame is similar to that reported in Ref. [32], and the lowest energy one, Si_5Li-a, shows the same Si_6 structure reported in this reference. The anion matches the structure reported by Yang et al. [44] with C_s symmetry, but the energy ordering is interchanged respect to the neutral series. It is important to note that Si_5Li-b$^-$ geometry relaxed to that of Si_5Li-c$^-$, the anion previously reported [44,25]. The Si–Li bond length decreased in 0.03 Å and 0.08 Å, for -a and -b anions, respect to the neutral species. The positive charged species keep the structure of the neutral ones, -a and -b, the first of them is a *TS* state and were previously reported in Ref. [25]. The Si–Li bond lengths decrease from 2.49 Å to 2.67 Å from neutral to cation structures.

Table 2
Calculated binding energies (E_b), adiabatic ionization energies (AIP), adiabatic electron affinity (AEA), polarisability per atom (α/n) and bond lengths for the Si_nLi (n = 2–7) clusters found by the MGAC–CPMD method.

Isomer		E_b (eV)	AIP (eV)	AEA (eV)	α/n (au)	Bond lengths (Å)	
						Si–Si	Si–Li
Si_2Li-a	(C_{2v})	1.916	6.86	1.68	59.57	2.104	2.565
Si_2Li-b	(C_s)	1.751	7.18	2.18	55.89	2.175	2.422
Si_3Li-a	(C_s)	2.439	7.46	1.89	41.04	2.305	2.497
Si_3Li-b	(C_1)	2.350	6.70	1.42	39.72	2.346	2.524
Si_4Li-a	(C_{2v})	2.771	6.80	1.66	37.90	2.348	2.652
Si_4Li-b	(C_s)	2.770	6.29	1.68	38.23	2.346	2.686
Si_4Li-c	(C_1)	2.763	6.27	1.20	39.38	2.326	2.499
Si_5Li-a	(C_{2v})	3.080	6.76	2.92	35.15	2.462	2.488
Si_5Li-b	(C_s)	3.080	6.22	2.25	35.20	2.474	2.498
Si_5Li-c	(C_1)	3.062	6.70	2.51	35.32	2.473	2.501
Si_6Li-a	(C_{2v})	3.234	6.46	1.77	33.01	2.441	2.619
Si_6Li-b	(C_s)	3.191	6.17	1.77	34.35	2.446	2.531
Si_6Li-c	(C_s)	3.191	6.16	1.99	33.47	2.449	2.602
Si_7Li-a	(C_{2v})	3.290	5.59	1.62	33.07	2.496	2.510
Si_7Li-b	(C_s)	3.257	6.59	1.94	34.19	2.446	2.608
Si_7Li-c	(C_1)	3.232	6.09	2.45	34.45	2.461	2.619

Our global search confirms that for the Si_6Li clusters the most stable neutral isomer and its derived negative anion have C_{2v} symmetry, as pointed out by Yang et al. [44]. We also found two additional stable structures, Si_6Li-b and Si_6Li-c, with their corresponding anions not previously reported. The energy difference between these two neutral isomers is 0.004 eV, and the structures differ in the lithium positions over the most stable Si_6Li isomer. The Si_6Li-a structure matches the best Si_7, as previously reported [32]. The relaxation of the three neutral structures produced only one isomer for the cation, which has not been previously reported.

For clusters with seven Si, our most stable neutral isomer matches the C_{2v} structure found in Refs. [21,44], but we found two other stable isomers, not previously reported, with C_s and C_1 symmetry, respectively. The difference between structures -a and -b is in the position of the Li atom. Si_7Li-a shows the same silicon structure as the most stable Si_7 cluster [32]. The corresponding anions interchange their energy order with respect to the uncharged species. The -a anion structure was not previously reported, as it is the case for -c [21,45]. The Si–Li bond length changed from 2.58 to 2.52 Å. The positive charged species show structures similar to those exhibited by the anions and the relative energy order between isomers is different from that of the neutral and anion species. The Si–Li bond length increased by 0.10 Å with respect to the neural isomers.

For clusters with eight or nine Si atoms, most of the structures found by MGAC/CPMD methodology are new structures. Only Si_8Li-a was re-obtained from the literature. Si_8Li-a, Si_8Li-d, Si_8Li-e, Si_8Li-f, Si_8Li-i and Si_8Li-k could have been found by replacement of one silicon atom by lithium in Si_9-a [45]. Si_8Li-g might have been found by replacement of one silicon atom by lithium in Si_9-b [46]. Si_8Li-b, Si_8Li-c and Si_8Li-h could be built by the addition of a lithium atom on Si_8-a [46]. The anions structures show almost the same structures as the neutral species with shorter bond distances. Si_8Li^--g and Si_8Li^--i are enantiomers. The most stable cation is Si_9Li^+-b and is similar to its neutral cluster. Instead Si_8Li^+-a is the last cation in the energy ordering, with C_{2v} symmetry and it is a transition state. The ordering for the other cations with similar structure to Si_8Li^+-a, is Si_8Li^+-k, Si_8Li^+-f, Si_8Li^+-e, and Si_8Li^+-d (*TS*). The bond average distance for cations grows up on 0.093 Å.

The neutral isomers of Si_9Li correspond to the addition of a lithium atom to Si_9-a [46]. The structure of Si_9Li-e, at 0.267 eV from Si_9Li-a is the only one previously reported. The anion Si_9Li^--e is the most stable among the charged species, with C_s symmetry. The cations are only three different structures in an narrow energy range of 0.090 eV.

The neutral isomers found by MGAC/CPMD with ten Si atoms correspond to the addition of one lithium atom into the Si_{10}-a [46], with the lithium atom in different positions. The most stable isomer, $Si_{10}Li$-a with C_s symmetry, was previously reported [44], and both kinds of charged species, cations and anions, have the same energy ranking as the neutral isomers. The anion $Si_{10}Li^-$-b is a transition state (*TS*).

Table 3
Calculated binding energies (E_b), the adiabatic ionization energies (AIP), the adiabatic electron affinity (AEA), polarisability per atom (α/n) and bond lengths for the Si_nLi (n = 8–10, 12) clusters found by the MGAC–CPMD method.

Isómero		E_b (eV)	AIP (eV)	AEA (eV)	α/n (au)	Bond lengths (Å)	
						Si–Si	Si–Li
Si_8Li-a	(C_{2v})	3.323	6.76	2.92	31.90	2.431	2.591
Si_8Li-b	(C_1)	3.312	6.22	2.25	33.04	2.453	2.574
Si_8Li-c	(C_1)	3.301	6.21	2.37	33.15	2.486	2.587
Si_8Li-d	(C_s)	3.293	6.67	2.61	32.39	2.444	2.644
Si_8Li-e	(C_1)	3.290	6.33	2.44	32.67	2.476	2.619
Si_8Li-f	(C_1)	3.289	6.44	2.52	32.37	2.497	2.484
Si_8Li-g	(C_1)	3.287	6.56	2.57	32.41	2.515	2.662
Si_8Li-h	(C_1)	3.278	5.99	2.55	33.65	2.491	2.617
Si_8Li-i	(C_1)	3.265	6.31	2.77	32.97	2.513	2.513
Si_8Li-j	(C_1)	3.262	6.25	2.53	33.25	2.481	2.547
Si_8Li-k	(C_s)	3.259	6.12	2.44	32.97	2.424	2.630
Si_9Li-a	(C_1)	3.386	5.87	2.83	31.81	2.434	2.582
Si_9Li-b	(C_1)	3.377	5.78	2.93	31.65	2.442	2.621
Si_9Li-c	(C_1)	3.374	5.84	2.94	32.25	2.442	2.538
Si_9Li-d	(C_1)	3.373	5.74	2.97	32.07	2.452	2.583
Si_9Li-e	(C_1)	3.359	5.70	3.16	32.32	2.437	2.562
$Si_{10}Li$-a	(C_s)	3.498	5.88	2.38	31.62	2.472	2.563
$Si_{10}Li$-b	(C_1)	3.490	5.80	2.38	31.31	2.480	2.592
$Si_{10}Li$-c	(C_s)	3.488	5.84	2.36	31.10	2.486	2.604
$Si_{10}Li$-d	(C_1)	3.481	5.76	2.43	31.28	2.468	2.575
$Si_{10}Li$-e	(C_1)	3.475	5.70	2.49	31.65	2.469	2.714
$Si_{10}Li$-f	(C_1)	3.475	5.96	2.46	32.14	2.480	2.564
$Si_{10}Li$-g	(C_1)	3.472	5.67	2.53	31.32	2.491	2.657
$Si_{12}Li$-a	(C_1)	3.489	5.81	2.86	31.64	2.468	2.616
$Si_{12}Li$-b	(C_1)	3.477	6.24	3.22	32.69	2.475	2.659
$Si_{12}Li$-c	(C_1)	3.437	6.02	2.81	31.73	2.499	2.585

MGAC/CPMD found three structures with twelve Si atoms, all with C_1 symmetry, from which only $Si_{12}Li$-a is stable; the other isomers are *TS*. $Si_{12}Li$-a and $Si_{12}Li$-b have a Si_{12}-a structure [47]. The anion structures are stable isomers but the energy ranking is $Si_{12}Li^-$-b, $Si_{12}Li^-$-a, $Si_{12}Li^-$-c. The Si–Li bond distances are reduced by 0.070 Å, 0.042 Å y 0.044 Å, with respect to the corresponding neutral isomers. The cation structures exhibit the same energy ordering than the neutral species, but the Si–Li distance goes from 2.616 Å to 2.696 Å for $Si_{12}Li^+$-a, 2.659 Å to 2.737 Å for $Si_{12}Li^+$-b, and 2.585 Å to 2.598 Å for $Si_{12}Li^+$-c.

Table 4 presents the incrustation energy, the HOMO–LUMO gaps for α and β electrons and the first vibrational mode for the most stable clusters found in this study. The incrustation energy, $EE = E[Si_nLi] - E[Si_n] - E[Li]$, where $E[Si_n]$ is the energy of the most stable silicon cluster [32], $E[Li]$ is the energy of a lithium atom and EE represents the energy necessary to add (or remove) a lithium atom to (from) Si_n (Si_nLi) clusters. For Si_5Li, which has one imaginary frequency, which corresponds to the second vibrational mode is given in Table 4.

Since sodium ($1s^22s^22p^61s^1$) and lithium ($1s^22s^1$) are alkali elements with similar electronic configuration we consider it useful to compare the electronic properties between Si–Li and Si–Na binary clusters. Geometric and electronic structures of silicon-sodium binary clusters have been studied by experimental and theoretical means by Kishi et al. [17,18]. The EE values evaluated for Si_nLi and those in Si_nNa ($n = 2–10$) reported by Yang et al. [44] are plotted in Fig. 6. The observed trends are very similar, but the EE energies are higher for Si_nLi than for Si_nNa. This means that the absorption of lithium on the surface of the silicon clusters is more stable than the sodium absorption.

Fig. 7 compares the EE energy and the adiabatic ionization energy (AIP) of Si_nLi clusters with the experimental values of the adiabatic electron affinity (AEA) of the corresponding Si_n clusters [45]. There are local minimum for $n = 2$, 4, 7, and local maximum for $n = 3$, 5, and 8 indicating that Si_nLi with $n = 3$, 5, and 8 are more stable than the other systems in the series. Furthermore, the AEA corresponding Si_n cluster shows size dependence similar to EE and API energies. The Si_n ($n = 3$, 5 and 8) clusters are specially stabilized, either by the adsorption of a Li atom or by the acceptance of one electron in excess. However, Si_n ($n = 2$, 4 and 7) clusters are stable structures when the cluster is neutral. As it was mentioned previously the AIPs compare successfully with the experimental data from Ref. [43], which reports values of 6.42–7.89 eV for Si_6Li, 5.65 ± 0.04 eV for Si_7Li, 6.42 eV for Si_8Li, values <7.89 eV for Si_9Li and 5.95 ± 0.05 for $Si_{10}Li$.

The dependence of the α and β gaps with cluster size is shown in Fig. 8 for the most stable isomers and are complementary; when

Table 4
Calculated embedding energies (EE), α and β energy gaps and first vibrational mode for the most stable Si_nLi ($n = 2–10$ and 12) clusters found by the MGAC–CPMD method.

Isomer		EE (eV)	α gap (eV)	β gap (eV)	Frequency (cm^{-1})
Si_2Li	(C_{2v})	2.64	3.47	2.02	417
Si_3Li	(C_s)	2.57	3.77	2.04	424
Si_4Li	(C_{2v})	2.01	2.64	3.29	384
Si_5Li	(C_s)	2.55	4.00	2.61	423
Si_6Li	(C_{2v})	2.17	3.05	2.50	398
Si_7Li	(C_{2v})	1.51	2.50	3.56	458
Si_8Li	(C_1)	2.07	2.67	1.84	413
Si_9Li	(C_1)	1.80	2.73	2.24	383
$Si_{10}Li$	(C_s)	1.87	2.24	3.13	445
$Si_{12}Li$	(C_1)	1.68	2.69	2.24	425

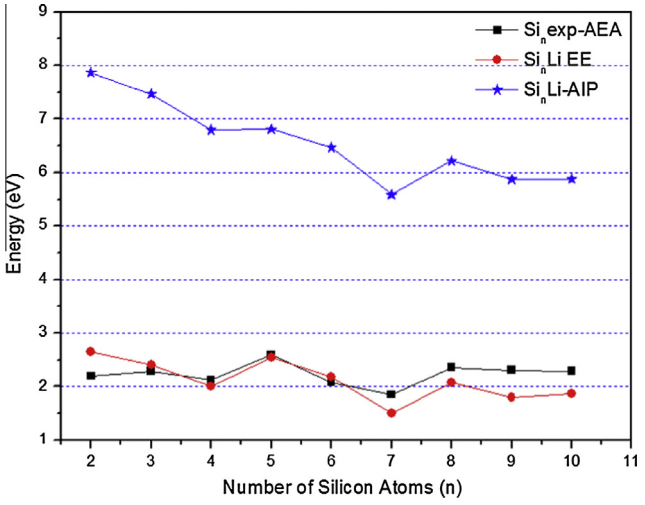

Fig. 7. The incrustation energy (EE) and the adiabatic ionization energy (AIP) of Si_nLi cluster and the adiabatic electron affinity (AEA) of Si_n cluster ($n = 2–10$) against the size (n) of the cluster.

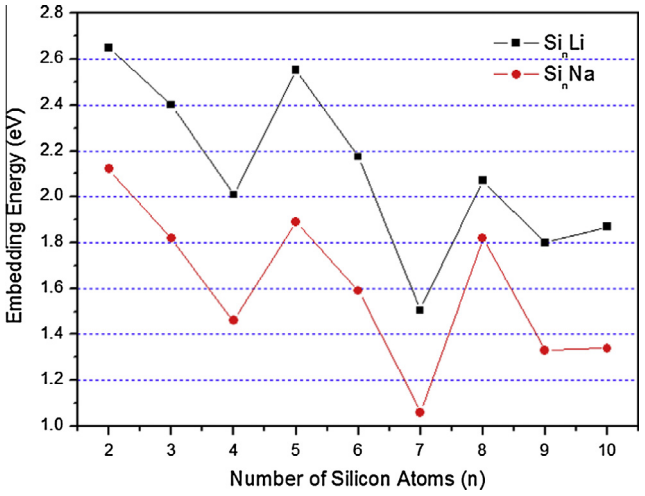

Fig. 6. The EE values evaluated for Si_nLi and Si_nNa ($n = 2–10$) by Yang et al. [44] are compared.

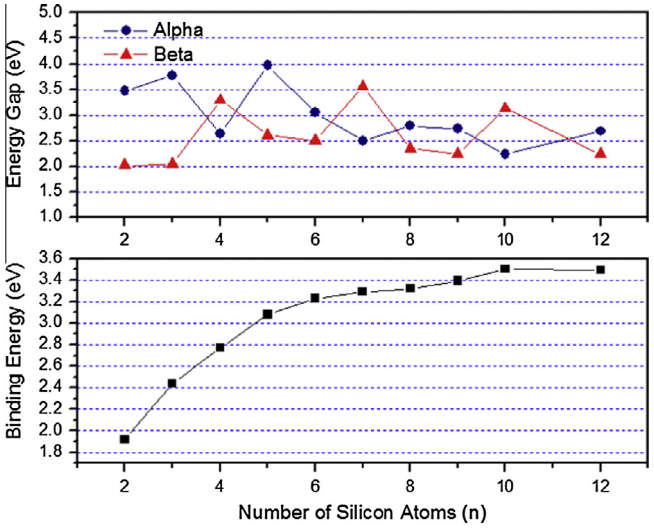

Fig. 8. HOMO–LUMO gap and E_b per atom for the most stable isomers Si_2Li–$Si_{10}Li$ and $Si_{12}Li$.

one α gap reaches a local maximum, β reaches a minimum, and vice versa. The behavior of the α gap is similar to EE and API of Si_nLi clusters. These results reinforce the observation from the analysis of their energies, indicating that Si_nLi with $n = 3,5,8$ are more stable than the other systems in the series.

The binding energy by atom (E_b) is plotted in the same figure as an upper graph. It increases from $n = 2$ to $n = 8$, but reaches a plateau, remaining almost constant for $n = 8$–12, indicating that for $n \geqslant 8$ the cluster is large enough to incorporate a lithium atom without an additional energy cost with respect to smaller silicon clusters.

Finally, the charge transfer due to the addition of a lithium atom to a Si_n cluster is considered by studying the natural charge on the lithium atom and the dipolar moment of the cluster for the most stable Si_nLi in function of the number, n, of silicon atoms. The dipolar moments for the corresponding anions and cations are plotted in the same figure. The dipolar moment reaches its maximum for Si_7Li and its minimum for Si_9Li (see Fig. 9). This behavior agrees with the shape of those clusters; Si_7Li looks enlarged in one direction and Si_9Li is nearly spherical. The dipolar moments are larger (lower) for cation (anions) than for neutral systems, in concordance with the behavior of the corresponding bond lengths. The dipolar moments of Si_nLi are plotted against the ratio between their inertia moment and the shorter inertia component for each cluster, at the right upper corner of the same figure. The natural charge on the lithium atom is plotted for the neutral Si_nLi's most stable isomers, and for the anion and cation corresponding to each other in Fig. 10. Both plots show that with respect to neutral and cation species, the natural charge on a lithium atom is smaller for anions. From the comparison between both figures, we conclude that the natural charge is sensible to geometry differences in the anions

In contrast with our results in Si_nCu clusters [36], the MGAC/CPMD global searches did not find any endohedral Si_nLi clusters. This is in spite of the fact that using the standard atomic radii such clusters are possible for clusters with more than eight silicon atoms. To further study this problem we performed local optimizations of an endohedral cluster of ten and twelve silicon atoms.

The initial structures for these optimizations where taken from Ref. [36], exchanging Cu by Li and from Ref. [30]. All these plausible endohedral cluster structures were locally optimized with the CPMD program and in the optimizations we observed that the Li atom was not ejected to the surface. The local optimizations successfully find stable endohedral Si_nLi clusters for $n = 10$, 12, but these clusters, depicted in Fig. 11, have relative energies with respect to the corresponding most stable clusters energies much higher than those from the clusters found by MGAC/CPMD global search, explaining why they are not found by the global search of MGAC populations.

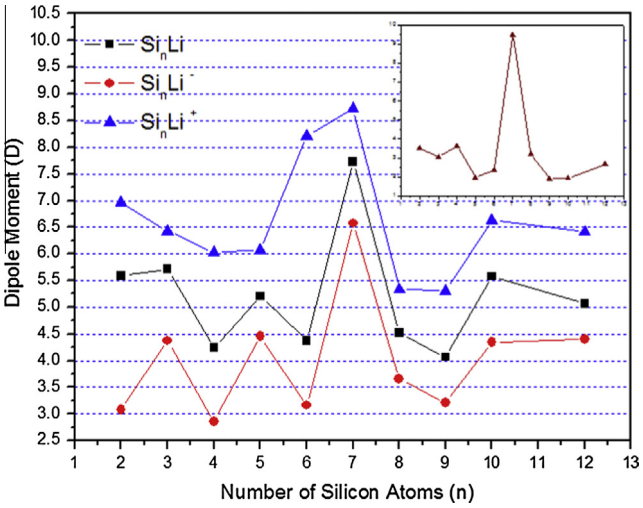

Fig. 9. Dipole moment for the most stable isomers Si_2Li–$Si_{10}Li$ and $Si_{12}Li$ and their corresponding anions and cations. The small plot at the upper corner shows the ratio between the Si_nLi inertia moment and the shorter component of this inertia moment against the number of silicon atoms.

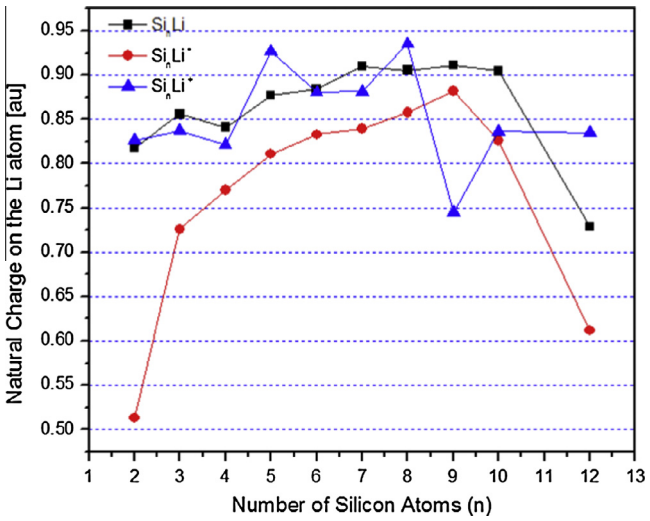

Fig. 10. Natural charge on a lithium atom for the neutral Si_nLi most stable isomers, and for their corresponding anion and cation.

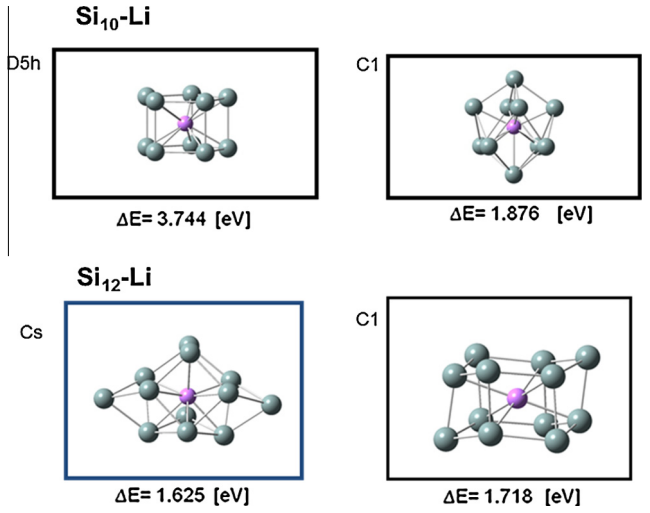

Fig. 11. Locally optimized endohedral clusters for $Si_{10}Li$ and $Si_{12}Li$. The initial structures for these optimizations where taken from Ref. [36], exchanging Cu by Li and from Ref. [30]. ΔE was calculated respect to the correspondent most stable Si_nLi ($n = 10,12$) found by the global MGAC/CPMD search.

4. Conclusions

The MGAC/CPMD method, with the Goedecker pseudopotential and PBE exchange correlation functional approach, was able to find several new structures for the Si_nLi ($n = 2$–10, 12) without employing any *a priori* information on the approximate conformation of the clusters. It is important to put into relevance that the structures reported have been found after a full search in the configurational space of each Si_nLi, taking into account only the number of silicon atoms in the cluster.

It is important to remark that we did not find any kind of Si_nLi cages; this is consistent with our local optimization of plausible cage structures for $n = 10$ and 12 that show energies much higher than those in the MGAC population. This behavior confirms that the absorption of lithium is difficult for cages of silicon and that there is a very low likelihood of finding endohedral lithium in silicon clusters.

The behavior of the α energy gap indicates that Si_nLi with $n = 3,5,8$ are more stable than the other systems in the series. The binding energy by atom (E_b) grows up from $n = 2$ to $n = 8$, and remains almost constant for $n = 8$–12. The reason is that for $n \geqslant 8$ the cluster is big enough to receive a lithium atom without additional cost with respect to smaller silicon clusters. The natural charge on lithium atom is sensible to geometry differences in the anions.

Acknowledgements

Financial support from University of Buenos Aires and CONICET and computational resources from the University of Utah Center for High Performance Computing are gratefully acknowledged.

Appendix A. Supplementary material

Supplementary data associated with this article can be found, in the online version, at http://dx.doi.org/10.1016/j.comptc.2013.09.019.

References

[1] J.L. Elkind, J.M. Alford, F.D. Weiss, R.T. Laaksonen, R.E. Smalley, FT-ICR probes of silicon cluster chemistry: the special behavior of Si_{39}^+, Chem. Phys. 87 (1987) 2397–2399.
[2] A.A. Shvartsburg, M.F. Jarrold, B. Liu, Z.Y. Lu, C.Z. Wang, K.M. Ho, Dissociation energies of silicon clusters: a depth gauge for the global minima on the potential energy surface, Phys. Rev. Lett. 81 (1998) 4616–4619.
[3] E.C. Honea, A. Ogura, C.A. Murray, K. Raghavachari, W.O. Sprenger, M.F. Jarrold, W.L. Brown, Raman spectra of size-selected silicon clusters and comparison with calculated structures, Nature (London) 366 (1993) 42–44.
[4] K. Raghavachari, C.M. Rohlfing, Bonding and stabilities of small silicon clusters: a theoretical study of Si_7–Si_{10}, J. Chem. Phys. 89 (1988) 2219–2234.
[5] C.M. Rohlfing, K. Raghavachari, Electronic structures and photoelectron spectra of Si_3^- and Si_4^-, J. Chem. Phys. 96 (1992) 2114–2117.
[6] K.M. Ho, A.A. Shavartsburg, B. Pan, Z.-Y. Lu, C.Z. Wang, J.G. Wacker, J.L. Fye, M.F. Jarrold, Structures of medium-sized silicon clusters, Nature (London) 392 (1998) 582–585.
[7] S.M. Beck, Mixed metal–silicon clusters formed by chemical reaction in a supersonic molecular beam: implications for reactions at the metal/silicon interface, J. Chem. Phys. 90 (1989) 6306–6312.
[8] M. Ohara, K. Koyasu, A. Nakajima, K. Kays, Geometric and electronic structures of metal (M)-doped silicon clusters (M = Ti, Hf, Mo and W), Chem. Phys. Lett. 371 (2003) 490–497.
[9] R.C. Binning, D.E. Bacelo, Structures and energetics of Be_nSi_n and $Be_{2n}Si_n$ ($n = 1$–4) clusters, J. Phys. Chem. A 109 (2005) 754–758.
[10] K. Koyasu, M. Mitsui, A. Nakajima, The selective formation of MSi_{16} (M = Sc, Ti, V), J. Am. Chem. Soc. 127 (2005) 4998–4999.
[11] J.B. Jaeger, T.D. Jaeger, M.A. Duncan, Photodissociation of metal–silicon clusters: encapsulated versus surface-bound metal, J. Phys. Chem. A 110 (2006) 9310–9314.
[12] C. Chan, H. Pain, G. Liu, K. Mcilwrath, X.F. Hang, R.A. Huggins, Y. Cui, High performance lithium battery anodes using silicon nanowires, Nat. Nanotechnol. 3 (2008) 31–35.
[13] B.A. Boukamp, G.C. Lesh, R.A. Huggins, All-solid lithium electrodes with mixed-conductor matrix, J. Electrochem. Soc. 128 (1981) 725–729.
[14] U. Kasavajjula, C. Wang, A.J. Appleby, Nano- and bulk-silicon-based insertion anodes for lithium–ion secondary cells, J. Power Source 163 (2007) 1003–1039.
[15] M. Ng, L. Shen, L. Zhou, S. Yang, V.B.C. Tan, Geometry dependent *I–V* characteristics of silicon nanowires, Nano Lett. 8 (2008) 3662–3667.
[16] K. Kaya, T. Sugioka, T. Taguwa, K. Hocino, A.Z. Nakajima, Sodium doped binary clusters I: Ionization potentials of Si_nNa_m clusters, Z. Phys. D. 26 (S) (1993) 201–203.
[17] R. Kishi, S. Iwata, A. Nakajima, K. Kaya, Geometric and electronic structures of silicon–sodium binary clusters I. Ionization energy of Si_nNa_m, J. Chem. Phys. 107 (1997) 3056–3070.
[18] R. Kishi, H. Kawamata, Y. Negishi, S. Iwata, A. Nakajima, K. Kaya, Geometric and electronic structures of silicon–sodium binary clusters. II. Photoelectron spectroscopy of $Si_nNa_m^-$ cluster anions, J. Chem. Phys. 107 (1997) 10029–10043.
[19] D.Y. Zubarev, A.N. Alexanrova, A.I. Boldyrev, L.F. Cui, X. Li, L.S. Wang, On the structure and chemical bonding of Si_{62}^- and Si_{62}^- in $NaSi_6^-$ upon Na^+ coordination, J. Chem. Phys. 124 (2006) 124305–124318.
[20] L.H. Lin, J.C. Yang, H.M. Ning, D.S. Hao, H.W. Fan, Silicon–sodium binary clusters Si_nNa ($n = 2$–10) and their anions: structures, thermochemistry, and electron affinities, J. Mol. Struct. (Theochem) 851 (2008) 197–206.
[21] H. Wang, W.C. Lu, Z.S. Li, C.C. Sun, Theoretical investigation on the adsorption of lithium atom on the Si_n cluster ($n = 2$–7), J. Mol. Struct. (Theochem) 730 (2005) 263–271.
[22] C. Sporea, F. Rabilloud, X. Cosson, A.R. Allouche, M. Aubert-Frecon, Theoretical study of mixed silicon–lithium clusters $Si_nLi_p^{(+)}$ ($n = 1$–6, $p = 1$–2), J. Phys. Chem. A 110 (2006) 6032–6038.
[23] C. Sporea, F. Rabilloud, A.R. Allouche, M. Aubert-Frecon, Ab initio study of neutral and charged $Si_nLi_p^{(+)}$ ($n<=6$, $p<=2$) clusters, J. Phys. Chem. A 110 (2006) 1046–1051.
[24] C. Sporea, F. Rabilloud, M. Aubert-Frecon, Charge transfers in mixed silicon–alkali clusters and dipole moments, J. Mol. Struct. (Theochem) 802 (2007) 85–90.
[25] D. Hao, J. Liu, J. Yang, A Gaussian-3 theoretical study of small silicon–lithium clusters: electronic structures and electron affinities of Si_nLi^- ($n = 2$–8), J. Phys. Chem. A 112 (2008) 10113–10119.
[26] L.A. Curtiss, K. Raghavachari, P.C. Redfern, V. Rassolov, J.A. Pople, Gaussian-3 (G3) theory for molecules containing first and second-row atoms, J. Chem. Phys. 109 (1998) 7764–7786.
[27] E.N. Koukaras, A.D. Zdetsis, P. Karamanis, C. Pouchan, A. Avramopoulos, M.G. Papadopoulos, Structural and static electric response properties of highly symmetric lithiated silicon cages: theoretical predictions, J. Comput. Chem. 33 (2012) 1068–1079.
[28] J. De Haeck, S. Bhattacharyya, H.T. Le, D. Debruyne, N.M. Tam, V.T. Ngan, E. Janssens, M.T. Nguyen, P. Lievens, Ionization energies of lithium doped silicon clusters, Phys. Chem. Chem. Phys. 14 (2012) 8542–8550.
[29] E. Osorio, V. Villalobos, J.C. Santos, K.J. Donald, G. Merino, W. Tiznado, Structure and stability of the Si_4Li_n ($n = 1$–7) binary clusters, Chem. Phys. Lett. 522 (2012) 67–71.
[30] C. Sporea, F. Rabilloud, Stability of alkali-encapsulating silicon cage clusters, J. Chem. Phys. 127 (2007) 164306–164312.
[31] M. Iwamatsu, Global geometry optimization of silicon clusters using the space-fixed genetic algorithm, J. Chem. Phys. 112 (2000) 10976–10983.
[32] C. Roberts, R.L. Johnston, N.T. Wilson, A genetic algorithm for the structural optimization of Morse clusters, Theor. Chem. Acc. 104 (2000) 123–130.
[33] V.E. Bazterra, M.B. Ferraro, J.C. Facelli, Modified genetic algorithm to model crystal structures. I. Benzene, naphthalene and anthracene, J. Chem. Phys. 116 (2002) 5984–5991.
[34] V.E. Bazterra, M. Cuma, M.B. Ferraro, J.C. Facelli, A General framework to understand parallel performance in heterogeneous systems, J. Parallel Distrib. Comp. 65 (2005) 48–57.
[35] O. Oña, V.E. Bazterra, M.C. Caputo, M.B. Ferraro, J.C. Facelli, Ab Initio global optimization of the structures of SinH, $n = 4$–10, using parallel genetic algorithms, Phys. Rev. A 72 (2005) 053205–053213.
[36] O. Oña, M.B. Ferraro, J.C. Facelli, Transition from exo- to endo- Cu absorption in CuSin clusters: a genetic algorithms density functional theory (DFT) study, J. Molec. Simul. 37 (2011) 678–688.
[37] R.L. Johnston, C. Roberts, Genetic Algorithms for the Geometry Optimization of Clusters and Nanoparticles, in: H.M. Cartwright, M. Sztandera (Eds.), Soft Computing Approaches in Chemistry, vol. 120, Springer-Verlag, Heildberg, 2003, pp. 161–204.
[38] E. Cantu-Paz, Efficient and Accurate Parallel Genetic Algorithms Series: Genetic Algorithms and Evolutionary Computation, vol. 1, Springer, Berlin, 2000.
[39] M. Parrinello, W. Andreoni, Computer code CPMD V3.9, http://www.cpmd.org/.
[40] S. Goedecker, J. Hutter, M. Teter, Separable dual-space Gaussian pseudopotentials, Phys. Rev. B 54 (1996) 1703–1710.
[41] J.P. Perdew, K. Burke, M. Ernzerhof, Generalized gradient approximation made simple, Phys. Rev. Lett. 77 (1996) 3865–3868.
[42] M.J. Frisch, G.W. Trucks, H.B. Schlegel, et al., Gaussian 03, Gaussian Inc., Wallingford, CT, 2003.
[43] N.M. Tam, V.T. Ngan, J. de Haeck, S. Bhattacharyya, H. Thuy Le, et al., Singly and doubly lithium doped silicon clusters: geometrical and electronic structures and ionization energies, J. Chem. Phys. 136 (2012) 024301–024311.
[44] J. Yang, L. Lin, Y. Zhang, A.F. Jalbout, Lithium–silicon Si_nLi ($n = 2$–10) clusters and their anions: structures, thermochemistry, and electron affinities, Theoret. Chem. Account 121 (2008) 83–90.
[45] V.E. Bazterra, O. Oña, M.C. Caputo, M.B. Ferraro, P. Fuentealba, J.C. Facelli, Modified genetic algorithms to model cluster structures in medium-size silicon clusters, Phys. Rev. A 69 (2004) 053202–053209.
[46] C. Xiao, F. Hagelberg, W.A. Lester Jr., Geometric, energetic, and bonding properties of neutral and charged copper-doped silicon clusters, Phys. Rev. B 66 (2002) 075425–075448.
[47] NIST Computational Chemistry Comparison and Benchmark Database, NIST Standard Reference Database Number 101 Release 15b, August 2011, Editor: Russell D. Johnson III. http://cccbdb.nist.gov/.